Limited Feedback MU-MIMO-OFDM Systems

A. Panajotović
Faculty of Electronic Engineering
University of Niš, Serbia
Email: aleksandra.panajotovic@elfak.ni.ac.rs

F. Riera-Palou and G. Femenias
Mobile Communications Group
University of the Balearic Islands, Spain
Email: {felip.riera,guillem.femenias}@uib.cat

***Abstract*—Practical precoding schemes inevitably have to deal with the problem of imperfect, rather than ideal, channel state information at the transmitter (CSIT). This impairment permeates all the processing steps conducted at the transmitter side and it also conditions the receiver design. This paper tackles the problem of designing multiuser MIMO-OFDM (MU-MIMO-OFDM) schemes when only limited feedback is available, with a particular emphasis on the case of IEEE 802.11ac. After deriving a statistical model for the interference caused by limited-feedback valid for various linear precoding schemes, it is shown how this information can be incorporated to the processes of user selection and link adaptation in the context of IEEE 802.11ac. Extensive simulation results are presented assessing the performance of the various limited-feedback designs and comparing them with their perfect CSIT counterparts.**

I. Introduction

The latest generation of wireless local area networks (WLANs), formally approved as IEEE 802.11ac [1], aims at a spectral efficiency approaching 43 bit/s/Hz, a figure that represents nearly a three-fold increase with respect to IEEE 802.11n. Such a dramatic improvement is achieved by, on one hand, including transmission modes based on 256-QAM modulation and, on the other hand, by using multiuser multiple-input multiple-output (MU-MIMO) techniques [2]. Among the many MU-MIMO techniques that have been proposed during the last decade, two of them stand out, namely, zero-forcing beamforming (ZFBF) [3] and block diagonalization (BD) [4]. Whereas ZFBF aims at canceling both inter- and intra-user interference, BD, in its original form, just cancels inter-user interference leaving intra-user processing to a subsequent beamforming/equalisation step. Remarkably, ZFBF and BD lead to the same solution for the case of single-antenna receivers, while for multi-antenna receivers, the most appropriate of these techniques, from a sum-rate point of view, changes depending on the operating SNR region [5].

The IEEE 802.11ac standard does not specify a particular form of MU-MIMO precoding although constrains this processing step to be implemented at the access point (AP) and to take a linear form, thus making ZFBF- or BD-based designs attractive alternatives for the downlink segment. What is actually specified in the standard is the accuracy of the channel information that the AP (transmitter) will have at hand to design the MU-MIMO precoder. In particular, IEEE 802.11ac defines feedback methods specifying how each user channel matrix can be efficiently conveyed to the transmitter under limited-feedback constraints [1].

In a MU-MIMO scheme, the set of users to be simultaneously served must be selected, as well as the number of data streams to be conveyed to each of them. Many user/streams selection methods have been proposed in the context of MU-MIMO ranging from the optimal, albeit computationally costly, exhaustive search to low-complexity suboptimal procedures (see for example [6] for some new results and an updated literature review). Unfortunately, direct application of these schemes to IEEE 802.11ac-like systems is not trivial as most methods are geared towards single-carrier architectures or OFDMA-based schemes where each subcarrier/resource block can be independently assigned. Notable exceptions are the works [7]–[9], where the semi-orthogonal user selection (SUS) algorithm introduced in [3] was adapted to multi-stream multicarrier users transmitting strictly using orthogonal frequency division multiplexing (OFDM) (i.e., frequency is not used for multiple access), resulting in the generalized multicarrier semiorthogonal user selection (GMSUS) algorithm, and directly applicable to IEEE.802.11ac. Unfortunately, all these references assume the availability of perfect channel state information at the transmitter (CSIT), and therefore, the presented results should be taken as upper bounds of what can be achieved in a practical system, where the quality of the CSIT is constrained by quantisation effects and/or delays. Very recently, authors in [10] have explored the effects limited feedback has on MU-MIMO when using BD in the context of IEEE 802.11ac. It is shown in [10] that limited-feedback dramatically impacts the overall system throughput performance since quantisation imperfections permeate different key processing stages such as the precoder design, the user selection process and the link adaptation (transmission mode selection). Regrettably, this quantisation analysis applies only to a MU-MIMO scheme based on the use of BD at the transmitter side with zero-forcing (ZF)-based receivers. In light of the results in [10], it is natural to wonder how the limited feedback will affect other popular MU-MIMO schemes so that a fair comparison can be established under realistic operating conditions.

This paper proposes a general framework to evaluate the performance of various linear multicarrier MU-MIMO schemes when taking into account that the accuracy of the channel information fedback to the AP is limited by finite-precision quantisation. The analysis is subsequently particularized to the quantisation specifications described in the IEEE 802.11ac standard. To this end, the statistical model for

the multiuser interference caused by the quantisation-related precoding imperfections introduced in [10] is expanded to encompass other popular designs such as those based on ZFBF [3] and coordinated BD (BD-SVD) [4]. The interference characterisation is then incorporated to the processes of user selection and link adaptation to optimize the overall throughput performance in the specific context of IEEE 802.11ac networks.

This introduction concludes with a brief notational remark. Vectors and matrices are denoted by lower- and upper-case bold letters, respectively, while non-bold letters are used for scalars, $\mathcal{D}(\boldsymbol{x})$ is a (block) diagonal matrix with $\boldsymbol{x}$ at its main diagonal, $|\mathcal{U}|$ is the cardinality of subset $\mathcal{U}$, $(.)^T$ and $(.)^H$ denote transpose and complex transpose, respectively, $\boldsymbol{I}_P$ is the $P \times P$ identity matrix, $\|\boldsymbol{a}\|$ denotes the Euclidean norm of a vector $\boldsymbol{a}$, and, $\mathbb{R}$ and $\mathbb{C}$ are the sets of real and complex numbers, respectively.

II. System model

Let us consider the downlink of a MU-MIMO-OFDM system where an AP equipped with N_T antennas communicates with a set $\mathcal{N} = \{1, \ldots, N_u\}$ of N_u MSs each equipped, without loss of generality, with the same number $N_R \leq N_T$ of receive antennas. The system operates over N_c OFDM subcarriers, out of which N_d are used to transmit user data while the rest correspond to pilots and guard bands. At a given scheduling period, and owing to the MU-MIMO-OFDM nature of the downlink transmission scheme, the AP conveys information to a subset $\mathcal{U} = \{u_1, \ldots, u_{|\mathcal{U}|}\} \subseteq \mathcal{N}$ of selected MSs, with MS u_i receiving L_{u_i} spatial streams, where it should hold that $L_{\mathcal{U}} \triangleq \sum_{i=1}^{|\mathcal{U}|} L_{u_i} \leq N_T$.

As the selected MS u_i has been allocated L_{u_i} spatial streams, the corresponding vector of transmitted symbols over subcarrier q can be expressed as $\boldsymbol{s}_{u_i}[q] = \begin{bmatrix} s_{u_i,1}[q] & \ldots & s_{u_i,L_{u_i}}[q] \end{bmatrix}^T$, where $s_{u_i,l}[q]$, for $l \in \{1, \ldots, L_{u_i}\}$, denotes a complex symbol drawn from the constellation characterizing the MCS allocated to MS u_i (as enforced by the IEEE 802.11ac standard, a single digital modulation scheme is selected for MS u_i, constant over all subcarriers and spatial streams).

After linear precoding, the transmitted symbol vector corresponding to the selected MS u_i can be expressed as

$$\boldsymbol{x}_{u_i}[q] = \boldsymbol{F}_{u_i}[q] \boldsymbol{P}_{u_i}^{1/2}[q] \boldsymbol{s}_{u_i}[q], \tag{1}$$

where $\boldsymbol{P}_{u_i}[q] = \mathcal{D}\left(\begin{bmatrix} P_{u_i,1}[q] & \ldots & P_{u_i,L_{u_i}}[q] \end{bmatrix}\right) \in \mathbb{R}^{L_{u_i} \times L_{u_i}}$ is the power allocation matrix, and $\boldsymbol{F}_{u_i}[q] = \begin{bmatrix} \boldsymbol{f}_{u_i,1}[q] & \ldots & \boldsymbol{f}_{u_i,L_{u_i}}[q] \end{bmatrix} \in \mathbb{C}^{N_T \times L_{u_i}}$ is the precoding matrix. The transmitted symbol vector corresponding to the N_u selected MSs can then be written as

$$\boldsymbol{x}_{\mathcal{U}}[q] = \sum_{i=1}^{|\mathcal{U}|} \boldsymbol{x}_{u_i}[q] = \boldsymbol{F}_{\mathcal{U}}[q] \boldsymbol{P}_{\mathcal{U}}^{1/2}[q] \boldsymbol{s}_{\mathcal{U}}[q], \tag{2}$$

where $\boldsymbol{F}_{\mathcal{U}}[q] = \begin{bmatrix} \boldsymbol{F}_{u_1}[q] & \ldots & \boldsymbol{F}_{u_{|\mathcal{U}|}}[q] \end{bmatrix} \in \mathbb{C}^{N_T \times L_{\mathcal{U}}}$ is the global precoding matrix affecting the selected MSs in $\mathcal{U}$, $\boldsymbol{P}_{\mathcal{U}}[q] = \mathcal{D}\left(\begin{bmatrix} \boldsymbol{P}_{u_1}[q] & \ldots & \boldsymbol{P}_{u_{|\mathcal{U}|}}[q] \end{bmatrix}\right) \in \mathbb{R}^{L_{\mathcal{U}} \times L_{\mathcal{U}}}$ is the power allocation matrix of all symbols transmitted on subcarrier q, and $\boldsymbol{s}_{\mathcal{U}}[q] = \begin{bmatrix} \boldsymbol{s}_{u_1}^T[q] & \ldots & \boldsymbol{s}_{u_{|\mathcal{U}|}}^T[q] \end{bmatrix}^T \in \mathbb{C}^{L_{\mathcal{U}} \times 1}$ is a vector containing the symbols simultaneously transmitted to the MSs in $\mathcal{U}$ on subcarrier q. Assuming a uniform power allocation among subcarriers, the power allocation matrices $\boldsymbol{P}_{\mathcal{U}}[q]$, for all q, must satisfy the constraint

$$\sum_{i=1}^{|\mathcal{U}|} \sum_{l=1}^{L_{u_i}} P_{u_i,l}[q] \|\boldsymbol{f}_{u_i,l}[q]\|^2 = \frac{P_T}{N_d}, \tag{3}$$

where P_T is the available power for all data subcarriers.

Assuming the use of a post-processing matrix $\boldsymbol{G}_{u_i}[q] \in \mathbb{C}^{L_{u_i} \times N_R}$, the post-processed signal $\boldsymbol{y}_{u_i}[q] \in \mathbb{C}^{L_{u_i} \times 1}$ at the output of the u_ith receiver can be expressed as

$$\begin{aligned} \boldsymbol{y}_{u_i}[q] &= \boldsymbol{G}_{u_i}[q] \boldsymbol{H}_{u_i}[q] \boldsymbol{x}_{\mathcal{U}}[q] + \boldsymbol{G}_{u_i}[q] \boldsymbol{n}_{u_i}[q] \\ &= \boldsymbol{G}_{u_i}[q] \boldsymbol{H}_{u_i}[q] \sum_{j=1}^{|\mathcal{U}|} \boldsymbol{F}_{u_j}[q] \boldsymbol{P}_{u_j}^{1/2}[q] \boldsymbol{s}_{u_j}[q] + \boldsymbol{\eta}_{u_i}[q], \end{aligned} \tag{4}$$

where $\boldsymbol{H}_{u_i}[q] \in \mathbb{C}^{N_R \times N_T}$ is the flat-fading MIMO channel characterizing the propagation conditions between the AP and the u_ith MS on subcarrier q, the vector $\boldsymbol{n}_{u_i}[q] \in \mathbb{C}^{N_R \times 1}$ is modeled as a zero-mean circularly symmetric additive Gaussian noise with covariance matrix $\boldsymbol{R}_n = \sigma_n^2 \boldsymbol{I}_{N_R}$, and $\boldsymbol{\eta}_{u_i}[q] \triangleq \boldsymbol{G}_{u_i}[q] \boldsymbol{n}_{u_i}[q] \in \mathbb{C}^{L_{u_i} \times 1}$ is a zero-mean circularly symmetric additive Gaussian noise vector with covariance matrix $\boldsymbol{R}_{\eta_{u_i}}[q] = \sigma_n^2 \boldsymbol{G}_{u_i}[q] \boldsymbol{G}_{u_i}^H[q]$.

As pre- and post-processing are performed on a subcarrier basis, the subcarrier index $[q]$ will be dropped from this point onwards in order to simplify notation. Let us use the singular value decomposition (SVD) to decompose the MIMO channel matrix $\boldsymbol{H}_{u_i}$ as

$$\begin{aligned} \boldsymbol{H}_{u_i} &= \begin{bmatrix} \tilde{\boldsymbol{U}}_{u_i} & \tilde{\boldsymbol{U}}_{u_i,s} \end{bmatrix} \begin{bmatrix} \tilde{\boldsymbol{\Sigma}}_{u_i} & \boldsymbol{0} \\ \boldsymbol{0} & \tilde{\boldsymbol{\Sigma}}_{u_i,s} \end{bmatrix} \begin{bmatrix} \tilde{\boldsymbol{V}}_{u_i}^H \\ \tilde{\boldsymbol{V}}_{u_i,s}^H \end{bmatrix} \\ &= \tilde{\boldsymbol{U}}_{u_i} \tilde{\boldsymbol{\Sigma}}_{u_i} \tilde{\boldsymbol{V}}_{u_i}^H + \tilde{\boldsymbol{U}}_{u_i,s} \tilde{\boldsymbol{\Sigma}}_{u_i,s} \tilde{\boldsymbol{V}}_{u_i,s}^H, \end{aligned} \tag{5}$$

where $\tilde{\boldsymbol{U}}_{u_i} \in \mathbb{C}^{N_R \times L_{u_i}}$ and $\tilde{\boldsymbol{U}}_{u_i,s} \in \mathbb{C}^{N_R \times (N_R - L_{u_i})}$ contain the left singular vectors associated, respectively, to the L_{u_i} largest and $(N_R - L_{u_i})$ smallest singular values of $\boldsymbol{H}_{u_i}$, $\tilde{\boldsymbol{\Sigma}}_{u_i} \in \mathbb{R}^{L_{u_i} \times L_{u_i}}$ and $\tilde{\boldsymbol{\Sigma}}_{u_i,s} \in \mathbb{R}^{(N_R - L_{u_i}) \times (N_T - L_{u_i})}$ are the matrices containing, respectively, the L_{u_i} largest and the $(N_R - L_{u_i})$ smallest singular values in their main diagonals, and $\tilde{\boldsymbol{V}}_{u_i}^H \in \mathbb{C}^{L_{u_i} \times N_T}$ and $\tilde{\boldsymbol{V}}_{u_i,s}^H \in \mathbb{C}^{(N_T - L_{u_i}) \times N_T}$ are the matrices containing the right singular vectors associated, respectively, to the L_{u_i} largest and the $(N_T - L_{u_i})$ smallest singular values of $\boldsymbol{H}_{u_i}$. Using this decomposition, the post-processing matrix $\boldsymbol{G}_{u_i}$ is designed as [3], [4]

$$\boldsymbol{G}_{u_i} = \begin{cases} \tilde{\boldsymbol{U}}_{u_i}^H & \text{ZFBF} \\ \boldsymbol{B}_{u_i} \tilde{\boldsymbol{U}}_{u_i}^H & \text{BD} \end{cases}, \tag{6}$$

where $\boldsymbol{B}_{u_i} \in \mathbb{C}^{L_{u_i} \times L_{u_i}}$ is a post-processing matrix used to manage the intra-user interference after block diagonalization.

Note that in both ZFBF and BD cases an *equivalent* MIMO channel matrix $\tilde{\boldsymbol{H}}_{u_i} \in \mathbb{C}^{L_{u_i} \times N_T}$ can be defined as

$$\tilde{\boldsymbol{H}}_{u_i} \triangleq \tilde{\boldsymbol{U}}_{u_i}^H \boldsymbol{H}_{u_i} = \tilde{\boldsymbol{\Sigma}}_{u_i} \tilde{\boldsymbol{V}}_{u_i}^H. \tag{7}$$

Thus, the post-processed signal $\boldsymbol{y}_{u_i}$ at the output of the u_ith receiver can be rewritten as

$$\boldsymbol{y}_{u_i} = \tilde{\boldsymbol{H}}_{u_i} \sum_{j=1}^{|\mathcal{U}|} \boldsymbol{F}_{u_j} \boldsymbol{P}_{u_j}^{1/2} \boldsymbol{s}_{u_j} + \boldsymbol{\eta}_{u_i}, \tag{8}$$

for the ZFBF case, with $\boldsymbol{R}_{\eta_{u_i}} = \sigma_n^2 \boldsymbol{I}_{L_{u_i}}$, and as

$$\boldsymbol{y}_{u_i} = \boldsymbol{B}_{u_i} \tilde{\boldsymbol{H}}_{u_i} \sum_{j=1}^{|\mathcal{U}|} \boldsymbol{F}_{u_j} \boldsymbol{P}_{u_j}^{1/2} \boldsymbol{s}_{u_j} + \boldsymbol{\eta}_{u_i}, \tag{9}$$

for the BD case, with $\boldsymbol{R}_{\eta_{u_i}} = \sigma_n^2 \boldsymbol{B}_{u_i} \boldsymbol{B}_{u_i}^H$.

III. Limited feedback designs

Due to the use of a constrained feedback channel between the MS u_i and the AP, the quantized CSI available at the AP can be modeled as[1]

$$\hat{\boldsymbol{H}}_{u_i} \triangleq \tilde{\boldsymbol{\Sigma}}_{u_i} \hat{\boldsymbol{V}}_{u_i}^H, \tag{10}$$

where $\hat{\boldsymbol{V}}_{u_i} = \tilde{\boldsymbol{V}}_{u_i} - \boldsymbol{E}_{u_i}$ is a quantized version of $\tilde{\boldsymbol{V}}_{u_i}$, and $\boldsymbol{E}_{u_i}$ is used to denote the quantisation noise, which is unknown at the transmitter side.

A. Zero-Forcing Beamforming

Using (2) and (8), the aggregated post-processed signal vector $\boldsymbol{y}_{\mathcal{U}} \in \mathbb{C}^{L_{\mathcal{U}} \times 1}$ at the output of the receivers of the set of selected MSs can be written in compact form as

$$\boldsymbol{y}_{\mathcal{U}} \triangleq \begin{bmatrix} \boldsymbol{y}_{u_1}^T & \dots & \boldsymbol{y}_{u_{|\mathcal{U}|}}^T \end{bmatrix}^T = \tilde{\boldsymbol{H}}_{\mathcal{U}} \boldsymbol{F}_{\mathcal{U}} \boldsymbol{P}_{\mathcal{U}}^{1/2} \boldsymbol{s}_{\mathcal{U}} + \boldsymbol{\eta}_{\mathcal{U}}, \tag{11}$$

where a global *equivalent* MIMO channel matrix $\tilde{\boldsymbol{H}}_{\mathcal{U}} \in \mathbb{C}^{L_{\mathcal{U}} \times N_T}$ has been defined as

$$\tilde{\boldsymbol{H}}_{\mathcal{U}} \triangleq \begin{bmatrix} \tilde{\boldsymbol{H}}_{u_i}^T & \dots & \tilde{\boldsymbol{H}}_{u_{|\mathcal{U}|}}^T \end{bmatrix}^T, \tag{12}$$

which can be rewritten in terms of the quantized global *equivalent* MIMO channel matrix $\hat{\boldsymbol{H}}_{\mathcal{U}} \triangleq \begin{bmatrix} \hat{\boldsymbol{H}}_{u_i}^T & \dots & \hat{\boldsymbol{H}}_{u_{|\mathcal{U}|}}^T \end{bmatrix}^T$ and the global quantisation noise matrix $\boldsymbol{E}_{\mathcal{U}} \triangleq \begin{bmatrix} \boldsymbol{E}_{u_i}^T & \dots & \boldsymbol{E}_{u_{|\mathcal{U}|}}^T \end{bmatrix}^T$ as

$$\hat{\boldsymbol{H}}_{\mathcal{U}} = \tilde{\boldsymbol{H}}_{\mathcal{U}} - \tilde{\boldsymbol{\Sigma}}_{\mathcal{U}} \boldsymbol{E}_{\mathcal{U}}, \tag{13}$$

where $\tilde{\boldsymbol{\Sigma}}_{\mathcal{U}} \triangleq \mathcal{D}\left(\begin{bmatrix} \tilde{\boldsymbol{\Sigma}}_{u_1} & \dots & \tilde{\boldsymbol{\Sigma}}_{u_{|\mathcal{U}|}} \end{bmatrix}\right)$.

As the aim of ZFBF is to cancel both the inter- and intra-user interference, one easy choice for $\boldsymbol{F}_{\mathcal{U}}$ if the AP had access to ideal CSI would be to use the pseudoinverse of $\tilde{\boldsymbol{H}}_{\mathcal{U}}$, as suggested by Yoo and Goldsmith in [3]. However, as the AP has only access to quantized CSI, the precoder can be obtained as the pseudoinverse of $\hat{\boldsymbol{H}}_{\mathcal{U}}$, that is,

$$\boldsymbol{F}_{\mathcal{U}} = \begin{bmatrix} \boldsymbol{F}_{u_1} & \dots & \boldsymbol{F}_{u_{|\mathcal{U}|}} \end{bmatrix} = \hat{\boldsymbol{H}}_{\mathcal{U}}^H \left(\hat{\boldsymbol{H}}_{\mathcal{U}} \hat{\boldsymbol{H}}_{\mathcal{U}}^H \right)^{-1}. \tag{14}$$

[1]As in [10], and in order to simplify the analysis, we assume that $\tilde{\boldsymbol{\Sigma}}_{u_i}$ is conveyed with a negligible quantisation error to the transmitter.

Thus, using (13) and (14) in (11) yields

$$\boldsymbol{y}_{u_i} = \boldsymbol{P}_{u_i}^{1/2} \boldsymbol{s}_{u_i} + \tilde{\boldsymbol{\Sigma}}_{u_i} \boldsymbol{E}_{u_i} \sum_{j=1}^{|\mathcal{U}|} \boldsymbol{F}_{u_j} \boldsymbol{P}_{u_j}^{1/2} \boldsymbol{s}_{u_j} + \boldsymbol{\eta}_{u_i}, \tag{15}$$

for all $u_i \in \mathcal{U}$, where the second term in the right hand side of these equations represents the interference leakage due to imperfect CSI.

B. Block Diagonalization

From (9) it can be easily deduced that BD requires that the matrices $\boldsymbol{F}_{u_i}$, for all $u_i \in \mathcal{U}$, satisfy

$$\bar{\tilde{\boldsymbol{H}}}_{u_i} \boldsymbol{F}_{u_i} = \boldsymbol{0}, \tag{16}$$

where $\bar{\tilde{\boldsymbol{H}}}_{u_i} \triangleq \begin{bmatrix} \tilde{\boldsymbol{H}}_{u_1}^T & \dots & \tilde{\boldsymbol{H}}_{u_{i-1}}^T & \tilde{\boldsymbol{H}}_{u_{i+1}}^T & \dots & \tilde{\boldsymbol{H}}_{u_{|\mathcal{U}|}}^T \end{bmatrix}^T$. A sufficient condition to satisfy this constraint is to design the precoders as $\boldsymbol{F}_{u_i} = \boldsymbol{N}_{u_i} \boldsymbol{A}_{u_i}$, where $\boldsymbol{N}_{u_i} \in \mathbb{C}^{N_T \times S_{u_i}}$ is a basis of the nullspace of $\bar{\tilde{\boldsymbol{H}}}_{u_i}$ and $\boldsymbol{A}_{u_i} \in \mathbb{C}^{S_{u_i} \times L_{u_i}}$ is an arbitrary matrix used to select the directions of transmission in case the dimension of the nullspace of $\bar{\tilde{\boldsymbol{H}}}_{u_i}$, denoted by S_{u_i}, is greater than L_{u_i}. However, as the AP has only access to imperfect quantized CSI, the precoding matrices $\boldsymbol{N}_{u_i}$, for all $u_i \in \mathcal{U}$, will be designed to satisfy

$$\bar{\hat{\boldsymbol{H}}}_{u_i} \boldsymbol{N}_{u_i} = \boldsymbol{0}, \tag{17}$$

where $\bar{\hat{\boldsymbol{H}}}_{u_i} \triangleq \begin{bmatrix} \hat{\boldsymbol{H}}_{u_1}^T & \dots & \hat{\boldsymbol{H}}_{u_{i-1}}^T & \hat{\boldsymbol{H}}_{u_{i+1}}^T & \dots & \hat{\boldsymbol{H}}_{u_{|\mathcal{U}|}}^T \end{bmatrix}^T$. Using the SVD, let us decompose $\bar{\hat{\boldsymbol{H}}}_{u_i}$ as

$$\bar{\hat{\boldsymbol{H}}}_{u_i} = \bar{\hat{\boldsymbol{U}}}_{u_i} \bar{\hat{\boldsymbol{\Sigma}}}_{u_i} \begin{bmatrix} \bar{\hat{\boldsymbol{V}}}_{u_i,1}^H \\ \bar{\hat{\boldsymbol{V}}}_{u_i,0}^H \end{bmatrix} \tag{18}$$

where $\bar{\hat{\boldsymbol{V}}}_{u_i,1} \in \mathbb{C}^{N_T \times (N_T - S_{u_i})}$ and $\bar{\hat{\boldsymbol{V}}}_{u_i,0} \in \mathbb{C}^{N_T \times S_{u_i}}$ contain, respectively, the right singular vectors associated to the non-null and the null singular values of $\bar{\hat{\boldsymbol{H}}}_{u_i}$, $\bar{\hat{\boldsymbol{\Sigma}}}_{u_i} \in \mathbb{R}^{(L_{\mathcal{U}} - L_{u_i}) \times N_T}$ is a diagonal matrix containing the singular values of $\bar{\hat{\boldsymbol{H}}}_{u_i}$ on its main diagonal, and $\bar{\hat{\boldsymbol{U}}}_{u_i} \in \mathbb{C}^{(L_{\mathcal{U}} - L_{u_i}) \times (L_{\mathcal{U}} - L_{u_i})}$ is a matrix formed by the left singular vectors of $\bar{\hat{\boldsymbol{H}}}_{u_i}$. The S_{u_i} columns of $\bar{\hat{\boldsymbol{V}}}_{u_i,0}$ form an orthonormal basis for the null space of $\bar{\hat{\boldsymbol{H}}}_{u_i}$ and thus, a good choice for the precoding matrix is $\boldsymbol{N}_{u_i} = \bar{\hat{\boldsymbol{V}}}_{u_i,0}$. Hence, using (13) and (17) in (9), the signal $\boldsymbol{y}_{u_i}$ at the output of the u_ith post-processing matrix can be rewritten as

$$\begin{aligned} \boldsymbol{y}_{u_i} = {} & \boldsymbol{B}_{u_i} \hat{\boldsymbol{H}}_{u_i} \bar{\hat{\boldsymbol{V}}}_{u_i,0} \boldsymbol{A}_{u_i} \boldsymbol{P}_{u_i}^{1/2} \boldsymbol{s}_{u_i} \\ & + \boldsymbol{B}_{u_i} \tilde{\boldsymbol{\Sigma}}_{u_i} \boldsymbol{E}_{u_i} \sum_{j=1}^{|\mathcal{U}|} \bar{\hat{\boldsymbol{V}}}_{u_j,0} \boldsymbol{A}_{u_j} \boldsymbol{P}_{u_j}^{1/2} \boldsymbol{s}_{u_j} + \boldsymbol{\eta}_{u_i}, \end{aligned} \tag{19}$$

where, as in the ZFBF case, the second term in the right hand side of this equation represents the interference leakage due to imperfect CSI.

After BD, the pre- and post-processing matrices $\boldsymbol{A}_{u_i}$ and $\boldsymbol{B}_{u_i}$ are used, respectively, to select the directions of transmission in case the nullspace of $\bar{\hat{\boldsymbol{H}}}_{u_i}$ is of dimension S_{u_i} greater than L_{u_i} and to diagonalize the equivalent channel. In order

to do so, two pre- and post-processing schemes are analyzed in this paper, namely, the BD-SVD and the BD-ZF strategies. Both strategies, as will be shown in the following paragraphs, need that the pre-processing matrices $\hat{\boldsymbol{V}}_{u_i,0}$, for all $u_i \in \mathcal{U}$, be conveyed to the corresponding MSs. This can be done by sending a second round of pre-processed pilots from the AP to the MSs where an (almost) error-free channel estimation can be performed (a assumed in [10]). Remarkably, note that this extra training round is avoided when using ZFBF.

a) BD-SVD scheme: In this case, the quantized equivalent block-diagonalized channel $\breve{\boldsymbol{H}}_{u_i} \triangleq \hat{\boldsymbol{H}}_{u_i}\hat{\boldsymbol{V}}_{u_i,0}$ at both the AP and MS u_i is decomposed using the SVD as

$$\breve{\boldsymbol{H}}_{u_i} = \breve{\boldsymbol{U}}_{u_i}\begin{bmatrix}\breve{\boldsymbol{\Sigma}}_{u_i} & \boldsymbol{0}\end{bmatrix}\begin{bmatrix}\breve{\boldsymbol{V}}_{u_i}^H \\ \breve{\boldsymbol{V}}_{u_i,0}^H\end{bmatrix} \tag{20}$$

where $\breve{\boldsymbol{U}}_{u_i} \in \mathbb{C}^{L_{u_i}\times L_{u_i}}$ and $\breve{\boldsymbol{V}}_{u_i} \in \mathbb{C}^{S_{u_i}\times L_{u_i}}$ contain, respectively the L_{u_i} left and right singular vectors associated to the L_{u_i} singular values of $\breve{\boldsymbol{H}}_{u_i}$, and $\breve{\boldsymbol{\Sigma}}_{u_i} \triangleq \text{diag}\left(\begin{bmatrix}\breve{\sigma}_{u_i,1} & \dots & \breve{\sigma}_{u_i,L_{u_i}}\end{bmatrix}\right) \in \mathbb{R}^{L_{u_i}\times L_{u_i}}$ is a diagonal matrix containing the corresponding L_{u_i} singular values on its main diagonal. Thus, a good choice for the pre- and post-processing matrices is $\boldsymbol{A}_{u_i} = \breve{\boldsymbol{V}}_{u_i}$ and $\boldsymbol{B}_{u_i} = \breve{\boldsymbol{U}}_{u_i}^H$. The resulting signal vector $\boldsymbol{y}_{u_i}$ at the output of the u_ith post-processing matrix can be rewritten as

$$\begin{aligned}\boldsymbol{y}_{u_i} &= \breve{\boldsymbol{\Sigma}}_{u_i}\boldsymbol{P}_{u_i}^{1/2}\boldsymbol{s}_{u_i} \\ &+ \breve{\boldsymbol{U}}_{u_i}^H\tilde{\boldsymbol{\Sigma}}_{u_i}\boldsymbol{E}_{u_i}\sum_{j=1}^{|\mathcal{U}|}\bar{\hat{\boldsymbol{V}}}_{u_j,0}\breve{\boldsymbol{V}}_{u_j}\boldsymbol{P}_{u_j}^{1/2}\boldsymbol{s}_{u_j} + \boldsymbol{\eta}_{u_i}.\end{aligned} \tag{21}$$

b) BD-ZF scheme: In this case, $\boldsymbol{A}_{u_i}$ is a non-null arbitrary matrix of dimension $(S_{u_i} \times L_{u_i})$, and the post-processing matrix $\boldsymbol{B}_{u_i}$ is designed as a ZF equalizer. Although the MS could design a ZF equalizer for the equivalent block-diagonalized channel $\tilde{\boldsymbol{H}}_{u_i}\hat{\boldsymbol{V}}_{u_i,0}$, it will be assumed in this paper that the ZF equalizer is designed for the estimated equivalent block-diagonalized channel $\breve{\boldsymbol{H}}_{u_i}$, that is,

$$\boldsymbol{B}_{u_i} = \left(\breve{\boldsymbol{H}}_{u_i}\boldsymbol{A}_{u_i}\right)^{-1}. \tag{22}$$

Using this equalizer it is guaranteed that the AP has a perfect knowledge of the post-processing filter matrices used at the MSs and thus will be able to accurately predict the system performance when selecting users and allocating power and spatial streams. The resulting signal vector $\boldsymbol{y}_{u_i}$ at the output of the u_ith post-processing matrix can then be rewritten as

$$\begin{aligned}\boldsymbol{y}_{u_i} &= \boldsymbol{P}_{u_i}^{1/2}\boldsymbol{s}_{u_i} + \left(\breve{\boldsymbol{H}}_{u_i}\boldsymbol{A}_{u_i}\right)^{-1}\tilde{\boldsymbol{\Sigma}}_{u_i}\boldsymbol{E}_{u_i} \\ &\times\sum_{j=1}^{|\mathcal{U}|}\bar{\hat{\boldsymbol{V}}}_{u_j,0}\boldsymbol{A}_{u_j}\boldsymbol{P}_{u_j}^{1/2}\boldsymbol{s}_{u_j} + \boldsymbol{\eta}_{u_i},\end{aligned} \tag{23}$$

C. Post-processing SINR

The post-processing SINR experienced by MS u_i on the lth spatial stream can be expressed, in general form, as

$$\gamma_{u_i,l} = \frac{\alpha_{u_i,l}P_{u_i,l}}{[\boldsymbol{R}_{u_i}]_{l,l} + \left[\boldsymbol{R}_{\eta_{u_i}}\right]_{l,l}}, \tag{24}$$

where

$$\alpha_{u_i,l} = \begin{cases}1 & \text{ZFBF, BD-ZF} \\ \breve{\sigma}_{u_i,l}^2 & \text{BD-SVD,}\end{cases} \tag{25}$$

$$\boldsymbol{R}_{\eta_{u_i}} = \begin{cases}\sigma_n^2\boldsymbol{I}_{L_{u_i}} & \text{ZFBF, BD-SVD} \\ \sigma_n^2\boldsymbol{B}_{u_i}\boldsymbol{B}_{u_i}^H & \text{BD-ZF,}\end{cases} \tag{26}$$

and

$$\boldsymbol{R}_{u_i} = \boldsymbol{D}_{u_i}\boldsymbol{E}_{u_i}\left(\sum_{j=1}^{|\mathcal{U}|}\boldsymbol{\Omega}_{u_j}\right)\boldsymbol{E}_{u_i}^H\boldsymbol{D}_{u_i}^H, \tag{27}$$

with

$$\boldsymbol{D}_{u_i} = \begin{cases}\tilde{\boldsymbol{\Sigma}}_{u_i} & \text{ZFBF} \\ \breve{\boldsymbol{U}}_{u_i}^H\tilde{\boldsymbol{\Sigma}}_{u_i} & \text{ZF-SVD} \\ \left(\breve{\boldsymbol{H}}_{u_i}\boldsymbol{A}_{u_i}\right)^{-1}\tilde{\boldsymbol{\Sigma}}_{u_i} & \text{BD-ZF,}\end{cases} \tag{28}$$

and

$$\boldsymbol{\Omega}_{u_j} = \begin{cases}\boldsymbol{F}_{u_j}\boldsymbol{P}_{u_j}\boldsymbol{F}_{u_j}^H & \text{ZFBF} \\ \bar{\hat{\boldsymbol{V}}}_{u_j,0}\breve{\boldsymbol{V}}_{u_j}\boldsymbol{P}_{u_j}\breve{\boldsymbol{V}}_{u_j}^H\bar{\hat{\boldsymbol{V}}}_{u_j,0}^H & \text{BD-SVD} \\ \hat{\boldsymbol{V}}_{u_j,0}\boldsymbol{A}_{u_j}\boldsymbol{P}_{u_j}\boldsymbol{A}_{u_j}^H\bar{\hat{\boldsymbol{V}}}_{u_j,0}^H & \text{BD-ZF.}\end{cases} \tag{29}$$

IV. Resource allocation with limited feedback

A. Estimating the post-processing SINR at the AP

Since the quantisation noise matrix $\boldsymbol{E}_{u_i}$ is unknown at the transmitter side, the interference-plus-noise covariance matrices $\boldsymbol{R}_{u_i}$ are random variables from the AP's point-of-view. Consequently, an estimated covariance matrix can be obtained at the transmitter side by averaging over the realisations of $\boldsymbol{E}_{u_i}$, that is,

$$\hat{\boldsymbol{R}}_{u_i} \triangleq \mathbb{E}_{\boldsymbol{E}_{u_i}}\{\boldsymbol{R}_{u_i}\} = \boldsymbol{D}_{u_i}\left(\sum_{j=1}^{|\mathcal{U}|}\boldsymbol{C}_{u_i,u_j}\right)\boldsymbol{D}_{u_i}^H, \tag{30}$$

where

$$\boldsymbol{C}_{u_i,u_j} \triangleq \mathbb{E}_{\boldsymbol{E}_{u_i}}\left\{\boldsymbol{E}_{u_i}\boldsymbol{\Omega}_{u_j}\boldsymbol{E}_{u_i}^H\right\}. \tag{31}$$

Hence, the AP estimation of the post-processing SINR experienced by MS u_i on the lth spatial stream is

$$\hat{\gamma}_{u_i,l} = \frac{\alpha_{u_i,l}P_{u_i,l}}{\left[\hat{\boldsymbol{R}}_{u_i}\right]_{l,l} + \left[\boldsymbol{R}_{\eta_{u_i}}\right]_{l,l}}, \tag{32}$$

B. Power allocation matrix

In order to maximize the estimated channel capacity per subcarrier, the diagonal components of the power allocation matrix $\boldsymbol{P}_{\mathcal{U}}$ can be obtained by solving the constrained convex optimisation problem

$$\max_{\boldsymbol{P}_{\mathcal{U}}}\sum_{i=1}^{|\mathcal{U}|}\sum_{l=1}^{L_{u_i}}\log_2\left(1 + \frac{\alpha_{u_i,l}P_{u_i,l}}{\left[\hat{\boldsymbol{R}}_{u_i}\right]_{l,l} + \left[\boldsymbol{R}_{\eta_{u_i}}\right]_{l,l}}\right) \tag{33}$$

subject to (3).

The analytical solution to this problem implies solving a rather involved non-linear system of equations. To simplify this procedure we propose to use an iterative water-filling algorithm in

Algorithm 1 : Multicarrier weighted capacity-based suboptimal user selection (MWCBSUS) algorithm

Initialize $L_u = 0$ for all $u \in \mathcal{N}$, and finish = false
Let $s = \arg\max_{u \in \mathcal{N}} \omega_u \sum_{q=1}^{N_d} \log_2(1 + \hat{\gamma}_{u,1})$
Set $\mathcal{U} = \{s\}$, $L_s = 1$, and $C_{\max} = \omega_s \sum_{q=1}^{N_d} \log_2(1 + \hat{\gamma}_{s,1})$
while $L_{\mathcal{U}} = \sum_{\forall u \in \mathcal{U}} L_u < N_T$ and finish = false **do**
  Set finish = true
  for Every $u \in \mathcal{N}$ such that $L_u < N_T$ **do**
    Let $\mathcal{U} = \mathcal{U} \cup \{u\}$, $L_u = L_u + 1$
    for Each $u \in \mathcal{U}$ and $q \in \{1, \ldots, N_d\}$ **do**
      Calculate pre- and post-processing matrices $\boldsymbol{F}_u[q]$, and $\boldsymbol{G}_u[q]$
      Use waterfilling to obtain $\boldsymbol{P}_u[q]$
    end for
    Evaluate $C = \sum_{i=1}^{|\mathcal{U}|} \omega_u \sum_{l=1}^{L_{u_i}} \sum_{q=1}^{Nd} \log_2(1 + \hat{\gamma}_{u_i,l}[q])$
    if $C > C_{\max}$ **then**
      $C_{\max} = C$, $s = u$, finish = false
    end if
    Set $\mathcal{U} = \mathcal{U} \backslash \{u\}$, $L_u = L_u - 1$
  end for
  if finish = false **then**
    $\mathcal{U} = \mathcal{U} \cup \{s\}$, $L_s = L_s + 1$
  end if
end while

which, to compute the allocated powers at iteration t, denoted as $P_{u_i,l}^{(t)}$ $\forall u_i, l$, the estimated interference covariance matrix is computed using the allocated powers calculated at iteration $(t-1)$, that is, $\hat{\boldsymbol{R}}_{u_i} \approx \hat{\boldsymbol{R}}_{u_i}^{(t-1)}$, and thus

$$P_{u_i,l}^{(t)} = \left(\frac{1}{\|\boldsymbol{f}_{u_i,l}\|^2 \mu^{(t)} \ln 2} - \frac{\left[\hat{\boldsymbol{R}}_{u_i}^{(t-1)}\right]_{l,l} + \left[\boldsymbol{R}_{\eta_{u_i}}\right]_{l,l}}{\alpha_{u_i,l}} \right)^+, \tag{34}$$

where $(x)^+ \triangleq \max\{0, x\}$, the water level $\mu^{(t)}$ is chosen to satisfy the constraint in (3), and $P_{u_i,l}^{(0)} = P_T/(N_d L_{\mathcal{U}})$ $\forall u_i, l$. Numerical experiments reveal that convergence takes place with few iterations.

C. User/stream selection

User/stream selection is the process whereby the selected user set $\mathcal{U} \subseteq \mathcal{N}$ and the number of data streams L_{u_i} allocated to each $u_i \in \mathcal{U}$ are determined. This process can be formulated as a multicarrier weighted sum-rate maximisation problem as

$$\max_{\left(\mathcal{U}, \{L_{u_i}\}_{i=1}^{|\mathcal{U}|}\right)} \omega_{u_i} \sum_{q=1}^{N_d} r_{u_i} \left[\left(\mathcal{U}, \{L_{u_i}\}_{i=1}^{|\mathcal{U}|}\right), q \right], \tag{35}$$
$$\text{subject to (3)}$$

where ω_{u_i} is the weight of user u_i in a given scheduling period, and $r_{u_i}\left[\left(\mathcal{U}, \{L_{u_j}\}_{j=1}^{|\mathcal{U}|}\right), q\right]$ is the supported data rate of user u_i on subcarrier q, with a scheduling decision $\left(\mathcal{U}, \{L_{u_j}\}_{j=1}^{|\mathcal{U}|}\right)$, which is related to the estimated SINRs $\hat{\gamma}_{u_i,l}$ in (32). The weights ω_{u_i} can be chosen based on different optimisation criteria resulting in a wide class of scheduling algorithms, including, among many others, the max-sum-rate (MSR) or the proportional fair (PF) [11].

The optimal solution to this problem would exhaustively evaluate the performance of all possible groupings $(\mathcal{U}, \{L_{u_i}\}_{i=1}^{|\mathcal{U}|})$. Obviously, even for a modest number of users in the system, this approach becomes computationally prohibitive, thus motivating the need for lower complexity suboptimal strategies. Examples of such feasible user selection procedures are the GMSUS algorithm [8], specifically designed to be used in conjunction with ZFBF, and the capacity-based suboptimal user selection (CBSUS) algorithm introduced in [12, Table I], originally designed for single-carrier architectures with with BD-based designs.

The GMSUS algorithm, described in detail in [8, Section IV.A], can be directly applied to our framework by simply taking into account that, instead of using $\tilde{\boldsymbol{H}}_{u_i}$, the quantized fed back version $\hat{\boldsymbol{H}}_{u_i}$ has to be considered, and the AWGN noise variance σ_η^2 must be substituted by the joint effects of AWGN and leakage interference, that is, $\left[\hat{\boldsymbol{R}}_{u_i}\right]_{l,l} + \left[\boldsymbol{R}_{\eta_{u_i}}\right]_{l,l}$.

Inspired by the CBSUS algorithm proposed by Shen *et al.* in [12], a multicarrier weighted capacity-based suboptimal user selection (MWCBSUS) has been designed and its processing steps are detailed in Algorithm 1.

D. Fast link adaptation (FLA)

Once users/streams have been chosen, and in light of the available estimated SINRs, an appropriate transmission mode must be selected, a process generically known as link adaptation. Fast link adaptation (FLA) refers to a specific flavour of link adaptation whereby the mode decisions are taken on a per-frame basis and relying on the available instantaneous estimated SINR information rather than on average (multi-frame) metrics. In this paper, the link adaptation process will be based on the FLA algorithm described in [8, Section V.A], suitably adapted to the limited feedback situation at hand. In fact, [8, eqs. (19)-(25)] can be directly used in our framework by substituting the instantaneous post-precessing SINRs $\gamma_{u_i,l}$, for all $u_i \in \mathcal{U}$ and $l \in \{1, \ldots, L_{u_i}\}$, by the quantized fed back versions $\hat{\gamma}_{u_i,l}$ shown in (32).

V. Limited feedback in IEEE 802.11ac

Developments presented in previous sections are general enough to be applicable to any MU-MIMO-OFDM system conforming to the assumptions taken into account when describing the system model. Nonetheless, since our focus is on IEEE 802.11ac, this section is dedicated to summarize the CSI acquisition mechanism described in the standard and the statistical characterisation of the interference leakage.

A. Acquiring CSI in IEEE 802.11ac

Although IEEE 802.11ac shares many features with IEEE 802.11n, some of them were modified in order to simplify the corresponding mechanisms. For instance, even though IEEE 802.11n supports both implicit and explicit feedback transmit beamforming, IEEE 802.11ac only supports explicit feedback beamforming that comprises, first, using null data packets (NDP) to send channel sounding sequences from the AP to the group of polled MSs and second, feeding back the estimated channel from the MSs to the AP using compressed (quantized) CSI [1, Sects. 8.3.1.20 and 9.31].

The channel sounding mechanism is initiated by the AP by transmitting a very high throughput (VHT) NDP announcement (NDPA) frame identifying the set of MSs potentially

going to be polled for feedback. The NDPA also contains information about the kind and form of the requested feedback. The NPDA is followed by a NDP frame, which is used by the MSs to estimate the corresponding MIMO channel. The first MS in the list of the NDPA sends quantized feedback information to the AP, and the remaining MSs (if any) report their quantized feedback CSI by responding to subsequent beamforming report polls.

Ideally, the message fed back from the MS u_i to the AP should contain the equivalent MIMO channel matrix $\tilde{\boldsymbol{H}}_{u_i} = \tilde{\boldsymbol{\Sigma}}_{u_i}\tilde{\boldsymbol{V}}_{u_i}^H$. The feedback of these non-compressed beamforming matrices, however, would require a large number of bits to represent the complex values with limited quantisation losses. Fortunately, as the beamforming matrix $\tilde{\boldsymbol{V}}_{u_i}$, containing the right eigenvectors associated to the largest singular values of the channel matrix, is unitary, polar coordinates may be used to reduce the number of bits required for beamforming weights feedback. In fact, $\tilde{\boldsymbol{V}}_{u_i}$ can be represented using Givens decomposition and the angles resulting from this decomposition are quantized and fed back to the AP where they are used to obtain the quantized version $\hat{\boldsymbol{V}}_{u_i}$ of the precoding matrix. Furthermore, the average SNR experienced by each spatial stream and each subcarrier is quantized and fed back to the AP where they are processed to obtain a quantized version of $\tilde{\boldsymbol{\Sigma}}_{u_i}$. As stated in the system model section, in order to simplify the analysis we assume in this paper that $\tilde{\boldsymbol{\Sigma}}_{u_i}$ is conveyed with a negligible quantisation error to the AP.

The unitary matrix $\tilde{\boldsymbol{V}}_{u_i} \in \mathbb{C}^{N_T \times L_{u_i}}$ is decomposed using Givens decomposition as [1]

$$\tilde{\boldsymbol{V}}_{u_i} = \left(\prod_{l=1}^{L_{u_i}} \boldsymbol{D}_{u_i,l} \prod_{n=l+1}^{N_T} \boldsymbol{G}_{u_i,l,n}^T\right) \tilde{\boldsymbol{I}}_{N_T,L_{u_i}}, \tag{36}$$

where $\tilde{\boldsymbol{I}}_{N_T,L_{u_i}}$ is a matrix containing the first L_{u_i} columns of $\boldsymbol{I}_{N_T}$, $\boldsymbol{D}_{u_i,l} = \text{diag}\left(\begin{bmatrix}\boldsymbol{1}_{l-1} & e^{j\boldsymbol{\Phi}_{\boldsymbol{u_i},\boldsymbol{l}}}\end{bmatrix}\right)$, with $\boldsymbol{\Phi}_{u_i,l} = \begin{bmatrix}\phi_{u_i,l,1} & \dots & \phi_{u_i,l,N_T-l+1}\end{bmatrix}$, and

$$\boldsymbol{G}_{u_i,l,n} = \begin{bmatrix} \boldsymbol{I}_{l-1} & & & & \\ & \cos\psi_{u_i,l,n} & & \sin\psi_{u_i,l,n} & \\ & & \boldsymbol{I}_{n-l-1} & & \\ & -\sin\psi_{u_i,l,n} & & \cos\psi_{u_i,l,n} & \\ & & & & \boldsymbol{I}_{N_T-n} \end{bmatrix}. \tag{37}$$

The angles $\psi_{u_i,l,n}$ and $\phi_{u_i,l,n}$ are quantized using uniform quantizers with b_ψ and b_ϕ bits, respectively. As $\psi_{u_i,l,n} \in [0, \pi/2]$ and $\phi_{u_i,l,n} \in [0, 2\pi]$, the quantized angles $\hat{\psi}_{u_i,l,n}$ and $\hat{\phi}_{u_i,l,n}$ can be expressed, respectively, as

$$\hat{\psi}_{u_i,l,n} = (2k+1)\delta \text{ if } \psi_{u_i,l,n} \in [2k\delta, 2(k+1)\delta], \tag{38}$$

for $k \in \left\{0, 1, \dots, 2^{b_\psi} - 1\right\}$, and

$$\hat{\phi}_{u_i,l,n} = (2k+1)\epsilon \text{ if } \psi_{u_i,l,n} \in [2k\epsilon, 2(k+1)\epsilon], \tag{39}$$

for $k \in \left\{0, 1, \dots, 2^{b_\phi} - 1\right\}$, where $\delta \triangleq \frac{\pi}{2^{b_\phi}}$ and $\epsilon \triangleq \frac{\pi}{2^{b_\psi+2}}$.

B. Statistical characterisation of the interference leakage

The processes of estimating the post-processing SINR, designing the per-subcarrier power allocation matrix, scheduling transmission to multiple users and performing fast link adaptation, described in subsections IV-A-IV-D, are all based on the estimation of the interference covariance matrices $\hat{\boldsymbol{R}}_{u_i}$ in (30) or, equivalently, the corresponding $\boldsymbol{C}_{u_i,u_j}$ matrices in (31) that, for mathematical convenience, can be rewritten as

$$\boldsymbol{C}_{u_i,u_j} = \begin{cases} \mathbb{E}_{\boldsymbol{V}_{u_i}|\hat{\boldsymbol{V}}_{u_i}}\left\{\boldsymbol{V}_{u_i}^H \boldsymbol{\Omega}_{u_j} \boldsymbol{V}_{u_i}\right\} & u_i \neq u_j \\ \mathbb{E}_{\boldsymbol{V}_{u_i}|\hat{\boldsymbol{V}}_{u_i}}\left\{\boldsymbol{V}_{u_i}^H \boldsymbol{\Omega}_{u_i} \boldsymbol{V}_{u_i}\right\} & \\ \quad - \mathbb{E}_{\boldsymbol{V}_{u_i}|\hat{\boldsymbol{V}}_{u_i}}\left\{\boldsymbol{V}_{u_i}^H\right\} \boldsymbol{\Omega}_{u_i} \hat{\boldsymbol{V}}_{u_i} & \\ \quad - \hat{\boldsymbol{V}}_{u_i}^H \boldsymbol{\Omega}_{u_i} \mathbb{E}_{\boldsymbol{V}_{u_i}|\hat{\boldsymbol{V}}_{u_i}}\{\boldsymbol{V}_{u_i}\} & u_i = u_j. \\ \quad + \hat{\boldsymbol{V}}_{u_i}^H \boldsymbol{\Omega}_{u_i} \hat{\boldsymbol{V}}_{u_i} & \end{cases} \tag{40}$$

To simplify the computation of these matrices, let us define $\varpi_{u_i,u_j} \triangleq \text{vec}\left(\mathbb{E}_{\boldsymbol{V}_{u_i}|\hat{\boldsymbol{V}}_{u_i}}\left\{\boldsymbol{V}_{u_i}^H \boldsymbol{\Omega}_{u_j} \boldsymbol{V}_{u_i}\right\}\right)$. In this case, using properties of the Kronecker product we have

$$\begin{aligned} \varpi_{u_i,u_j} = &\left(\tilde{\boldsymbol{I}}_{N_T,L_{u_i}}^T \otimes \tilde{\boldsymbol{I}}_{N_T,L_{u_i}}^H\right) \\ &\times \left(\prod_{l=1}^{L_{u_i}} \boldsymbol{R}_{u_i,l}^T \prod_{n=l+1}^{N_T} \boldsymbol{W}_{u_i,l,n}\right)^T \text{vec}\left(\boldsymbol{\Omega}_{u_j}\right), \end{aligned} \tag{41}$$

where the matrices

$$\boldsymbol{R}_{u_i,l} \triangleq \mathbb{E}_{\phi_{u_i,l}|\hat{\phi}_{u_i,l}}\left\{\boldsymbol{D}_{u_i,l}^T \otimes \boldsymbol{D}_{u_i,l}^H\right\} \tag{42}$$

and

$$\boldsymbol{W}_{u_i,l,n} \triangleq \mathbb{E}_{\psi_{u_i,l,n}|\hat{\psi}_{u_i,l,n}}\left\{\boldsymbol{G}_{u_i,l,n}^T \otimes \boldsymbol{G}_{u_i,l,n}^H\right\} \tag{43}$$

can be approximated in closed form using [10, eqs. (29)-(38)], where it is assumed that all the angles $\phi_{u_i,l}$ and $\psi_{u_i,l,n}$ are independent. Furthermore, using the same assumption,

$$\begin{aligned} \mathbb{E}_{\boldsymbol{V}_{u_i}|\hat{\boldsymbol{V}}_{u_i}}\{\boldsymbol{V}_{u_i}\} = &\left(\prod_{l=1}^{L_{u_i}} \mathbb{E}_{\phi_{u_i,l}|\hat{\phi}_{u_i,l}}\{\boldsymbol{D}_{u_i,l}\}\right. \\ &\left.\times \prod_{n=l+1}^{N_T} \mathbb{E}_{\psi_{u_i,l,n}|\hat{\psi}_{u_i,l,n}}\left\{\boldsymbol{G}_{u_i,l,n}^T\right\}\right) \tilde{\boldsymbol{I}}_{N_T,L_{u_i}}, \end{aligned} \tag{44}$$

that can also be obtained in closed form using [10, eqs. (31)-(34)].

VI. Numerical results and discussion

This section presents simulation results obtained using parameters drawn from IEEE 802.11ac standard, namely, the system operates at a 5.25 GHz carrier frequency over a bandwidth of $W = 20$ MHz that has been divided into $N_c = 64$ subcarriers out of which $N_d = 52$ carry data. The AP is equipped with $N_T = 4$ transmit antennas and all MSs have $N_R = 2$ receive antennas. For the simulations shown here, Channel profile B from [13] is used, suitably modified in accordance to [14] to adapt it to the IEEE 802.11ac peculiarities.

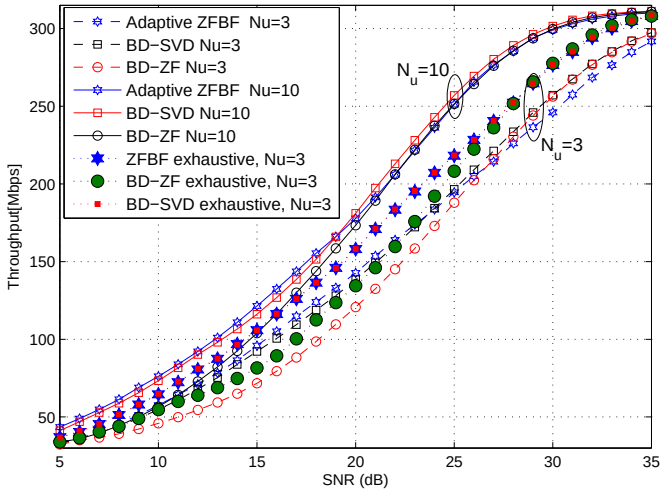

Fig. 1. Throughput comparison between ZFBF and BD-based MU-MIMO-OFDM applying appropriate user selection algorithms under perfect CSIT.

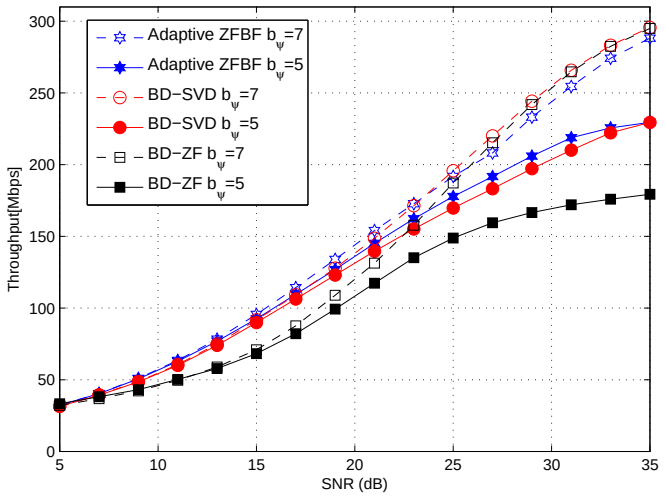

Fig. 2. Throughput of the limited feedback BD-ZF MU-MIMO-OFDM for $N_u = 3$ users.

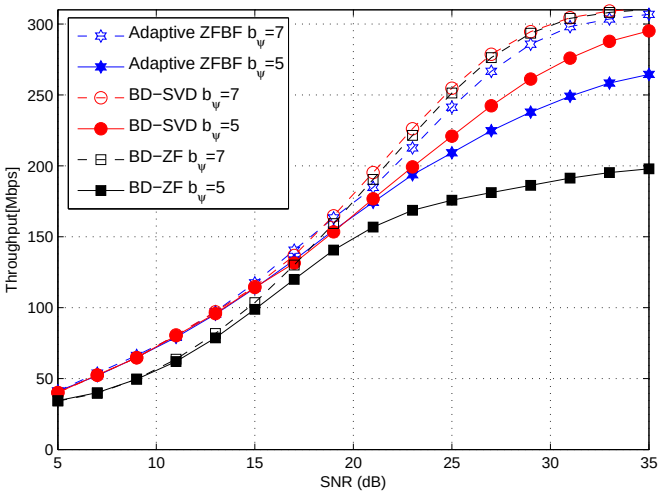

Fig. 3. Throughput of the limited feedback BD-ZF MU-MIMO-OFDM for $N_u = 10$ users.

This channel profile is representative of an environment with little-to-moderate frequency selectivity, as it is typically case in small office and houses. FLA-related parameters have been adopted from [8] to ensure a target PER of $PER_0 = 0.1$ with an outage probability of $P_{\text{out}} = 0.05$. A convolutional encoder with base code rate $R_c = 1/2$ and generator polynomials $g = [133, 171]_8$ has been used, while packet length is fixed to L=1664 bits. To better illustrate the behaviour of the considered algorithms, all the results shown here have been obtained in a homogeneous scenarios characterized by all users lying on a circumference centered on the AP, and thus all experiencing the same average SNR. Three different schemes are compared, namely, (adaptive) GMSUS-ZFBF, Multicarrier CBMUS-BD-SVD and Multicarrier CBMUS-BD-ZF, noting that for each precoding technique, BD-based or ZF-based, the corresponding suboptimal low-complexity user selection method has been applied (MWCBSUS and (adaptive) GMSUS, respectively).

As a baseline result, Fig. 1 compares the throughput performance of ZFBF and BD-based MU-MIMO schemes under the assumption of perfect CSIT and for different number of users in the system. For comparative purposes, results when conducting an exhaustive search[2] are also shown. The first obvious point to note is the benefit of having more users in the system ($N_u = 10$ rather than $N_u = 3$) owing to the larger multiuser diversity. Also note that all curves tend to a throughput of 312 Mbps, the limit achieved when the highest transmission mode (256-QAM, 5/6), achieving a throughput of 78 Mbps, can be configured on the four transmitted streams. Focusing solely on the precoding, results obtained using exhaustive search for $N_u = 3$ users reveal that BD-SVD and ZFBF virtually attain the same throughput performance whereas the utilisation of a ZF at the receiver, which unavoidably leads to noise enhancement, causes a degradation in throughput, specially at low SNRs (i.e., where noise enhancement is more severe). Pretty much the same effect can be observed when using suboptimal user selection for either $N_u = 10$ or $N_u = 3$ although the degradation caused by ZF equalisation becomes somewhat masked by an increased multiuser diversity gain that allows users experiencing better instantaneous SNRs to be selected.

Figures 2 and 3 show the performance of the different precoding schemes for 3 and 10 users, respectively, when considering, as specified in IEEE 802.11ac, the use of 5 and 7 bits for the quantisation of the angles $\psi_{i_i,l,n}$ (and correspondingly 7 and 9 bits for the quantisation of b_ϕ)[3]. It should be pointed out that $b_\psi = 7$ results in a negligible performance degradation with respect to the perfect CSIT assumption shown in Fig. 1. Focusing first on the three-user

[2]Exhaustive search results are only shown for $N_u = 3$ as for N_u values larger than 5 it is computationally infeasible.

[3]Note that $\psi_{i_i,l,n} \in [0, \pi/2]$ and $\phi_{i_i,l,n} \in [0, 2\pi]$ hence choosing $b_\phi = b_\psi + 2$ ensures the same accuracy in the quantisation of both angles [10].

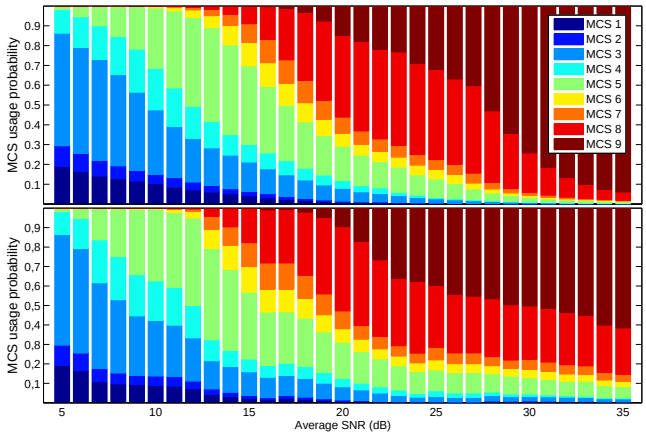

Fig. 4. Frequency of occurrence of the different transmission modes for N_u= 10 for $b_\psi = 7$ (upper plot) and $b_\psi = 5$ (lower plot).

results, it is clear that, parallelizing perfect CSIT results, the BD-ZF approach leads to rather worse results than the BD-SVD or ZFBF at low to moderate SNRs, whereas BD-SVD and ZFBF attain very similar performance over the whole SNR range. Remarkably, the losses associated to a coarse quantisation ($b_\psi = 5$) are only visible at large SNRs, thus revealing that at low SNRs, performance is not limited by imperfect CSIT but rather by the environment conditions (i.e., path loss, shadowing). Turning now our attention to the 10-user scenario (Fig. 3), it can be noticed how quantisation effects are not as deleterious as in the three-user case, thus suggesting that the increased level of multiuser diversity somehow masks limited feedback losses. Figure 4, plotting the probability of usage of every transmission mode for $b_\psi = 7$ (upper plot) and $b_\psi = 5$ (lower plot), helps to understand the degradation observed in the throughput results: note that the mode usage distribution follows the same trend for both quantisation levels, however, as the SNR increases, the setup with more accurate feedback is able to exploit the availability of the highest transmission modes (MCS 9) much more frequently. In particular, for $b_\psi = 5$ MCS 9 is selected 60% of the time for SNR=35 dB, while when $b_\psi = 7$ is selected 95% of the time.

VII. Conclusion

This paper has presented a comprehensive study of the effects limited feedback has in MU-MIMO-OFDM architectures with special emphasis on the case of IEEE 802.11ac. To this end, a general model to statistically characterize the (multiuser) interference arising from the use of precoders designed using quantised feedback information has been developed. This model is general enough to encompass the use of various ZFBF- and BD-based designs and it allows the effects of imperfect CSIT to be incorporated to the critical processes of user and transmission mode selection. Numerical results have shown that the most accurate quantisation level contemplated in IEEE 802.11ac ($b_\psi = 7$,$b_\phi = 9$) barely affect system performance with respect to that achieved under a perfect CSIT assumption. In contrast, coarser quantisation ($b_\psi = 5$, $b_\phi = 7$) unavoidably leads to a throughput degradation that is specially noticeable when only a few users are active in the network (i.e. an increased level of multiuser diversity somehow compensates quantisation losses) and/or the system operates at low SNRs. Both BD-based and ZFBF-based seem to be equally affected by limited feedback although ZFBF consistently and significantly outperforms BD-based techniques at low SNRs. Furthermore, it is remarkable that ZFBF just requires of a single training round to design the transmitter and receiver filters whereas BD-based approaches inevitably require of a double training phase, thus complicating their practical implementation.

Acknowledgements

Work supported by MINECO (Spanish Government) and FEDER under projects TEC2011-25446 and TEC2014-59255-C3-2-R.

References

[1] IEEE Computer Society, "IEEE Standard for Information technology–Telecommunications and information exchange between systems – Local and metropolitan area networks – Specific requirements. Part 11: Wireless LAN MAC and PHY Specifications. Amendment 4: Enhancements for Very High Throughput for Operation in Bands below 6 GHz," IEEE Std 802.11ac-2013, December 2013.

[2] D.Gesbert, M. Kountouris, R. Heath, C.-B. Chae, and T. Salzer, "Shifting the MIMO paradigm," *IEEE Signal Processing Mag.*, vol. 24, no. 5, Sept. 2007.

[3] T. Yoo and A. Goldsmith, "On the optimality of multiantenna broadcast scheduling using zero-forcing beamforming," *IEEE JSAC*, vol. 24, no. 3, pp. 528–541, March 2006.

[4] Q. Spencer, A. Swindlehurst, and M. Haardt, "Zero-forcing methods for downlink spatial multiplexing in multiuser MIMO channels," *IEEE Trans. on Signal Processing*, vol. 52, no. 2, pp. 461–471, Feb. 2004.

[5] R. Chen, Z. Shen, J. G. Andrews, and R. W. Heath, "Multimode transmission for multiuser MIMO systems with block diagonalization," *IEEE Trans. on Signal Processing*, vol. 56, no. 7, pp. 3294–302, 2008.

[6] M. Wang, T. Samarasinghe, and J. Evans, "Optimizing user selection schemes in vector broadcast channels," *IEEE Trans. on Communications*, vol. 63, no. 2, pp. 565–577, Feb 2015.

[7] M. Esslaoui, F. Riera-Palou, and G. Femenias, "Opportunistic multiuser MIMO for OFDM networks," in *8th International Workshop on Multi-Carrier Systems Solutions (MC-SS)*, May 2011, pp. 1–5.

[8] A. Panajotovic, F. Riera-Palou, and G. Femenia, "Adaptive uniform channel decomposition in MU-MIMO-OFDM: Aplication to ieee 802.11ac," *IEEE Transactions on Wireless Communications*, vol. 14, no. 5, pp. 2896–2910, 2015.

[9] M. Esslaoui, F. Riera-Palou, and G. Femenias, "A fair MU-MIMO scheme for IEEE 802.11ac," in *Wireless Communication Systems (ISWCS),2012 International Symposium on*, 2012, pp. 1049–1053.

[10] A. Rico-Alvariño and R. W. Heath, "Learning-based adaptive transmission for limited feedback multiuser MIMO-OFDM," *IEEE Transactions on Wireless Communications*, vol. 13, no. 7, pp. 3806–3820, Jul. 2014.

[11] G. Femenias, B. Dañobeitia, and F. Riera-Palou, "Unified approach to cross-layer scheduling and resource allocation in OFDMA wireless networks," *EURASIP Journal on Wireless Communications and Networking*, vol. 2012, no. 1, pp. 1–19. [Online]. Available: http://dx.doi.org/10.1186/1687-1499-2012-145

[12] Z. Shen, R. Chen, J. G. Andrews, R. W. H. Jr., and B. L. Evans, "Low complexity user selection algorithms for multiuser MIMO systems with block diagonalization," *IEEE Trans. on Signal Processing*, vol. 54, no. 9, pp. 3658–3663, Sep. 2006.

[13] J. Kermoal, L. Schumacher, K. Pedersen, P. Mogensen, and F. Frederiksen, "A stochastic MIMO radio channel model with experimental validation," *IEEE Journal on Selected Areas in Communications*, vol. 20, no. 6, pp. 1211–1226, Aug. 2002.

[14] IEEE Computer Society, "TGac Channel Model Addendum Supporting Material," IEEE 802.11-09/0569r0, May 2009.